OPEN ACCESS
Journal of Multidisciplinary Applied Natural Science Vol. 5 No. 2 (2025) https://doi.org/10.47352/jmans.2774-3047.254
Check for updates
Research Article

# Enhancing Supercapacitor Cell Capacitance through Liquid-Phase Exfoliation Synthesis of Graphene

Buky Wahyu Pratama, Haris Suhendar, Wipsar Sunu Brams Dwandaru, and Iman Santoso*

| Received : August 24, 2024 | Revised : December 2, 2024 | Accepted : December 21, 2024 | Online : March 26, 2025 |
|---|---|---|---|

**Abstract**
Our study investigates the remarkable capacitance performance of a supercapacitor cell featuring electrodes synthesized through the liquid-phase exfoliation (LPE) method using environmentally friendly linear alkylbenzene sulfonate (LAS) surfactant. We explored different synthesis temperatures (15, 30, and 90 °C) to evaluate their impact on reducing sonication time. The electrodes, created by drop-casting graphene onto a silver plate substrate and heated at 50 °C, demonstrated exceptional cyclic voltammetry (CV) and charging-discharging (CD) results. Notably, the graphene synthesized at 90 °C exhibited a maximum capacitance of 59 F/g at a 13 mV/s scan rate in a 1.3 M KOH electrolyte gel, leading to superior energy density as shown in the Ragone plot. Our findings highlight the crucial role of increased synthesis temperature in LPE, enhancing supercapacitor cells through the expansion of $sp^2$-ordered grain size, evident in the Raman shift data's ID/IG increase.

**Keywords:** supercapacitor, graphene, liquid-phase exfoliation, temperature, linear alkylbenzene sulfonate

## 1. INTRODUCTION

Supercapacitors, renowned for their high-power density, maintenance-free nature, and prolonged life cycles, play a pivotal role in modern energy storage systems [1]-[3]. The key determinant of supercapacitor performance is capacitance, intricately linked to electrode surface area [2][4]. Among the variety of materials employed for electrodes, the carbon family, particularly graphene, stands out due to its extensive surface area and superior conductivity [5]-[7]. Graphene, a two-dimensional carbon allotrope, boasts remarkable mechanical, electronic, and thermal properties, making it an ideal candidate for supercapacitor applications [7].

While various methods for synthesizing graphene exist, each has merits and drawbacks. Techniques like mechanical exfoliation, chemical vapor deposition, and epitaxial growth are efficient but limited to small-scale production [8]-[11]. In contrast, liquid-phase exfoliation (LPE) and chemical reduction of graphene oxide (CGO) are preferred for large-scale synthesis due to cost-effectiveness, although they introduce defects and impurities [12][13], such as oxides, carboxyl, hydroxyl, and carbonyls [9][14], adversely affecting graphene's properties [15]. The impurity can be reduced through techniques such as thermal reduction, adding hydrazine, and microwave reduction [16]-[18], although hydrazine poses environmental concerns due to its toxicity. Moreover, the oxide groups still exist in graphene sheets [19].

LPE involves exfoliating graphite into graphene sheets using ultrasonic vibration in a liquid phase. Ultrasonic vibrations cause bubbles to form in the solution. Which grow over time, eventually creating hot spots with high pressure that break the van der Waals bonds within the graphitic layers [13]. Organic solvents, such as NMP and DMF, along with ionic and non-ionic surfactants, are commonly used in LPE method [13][20]. However, the method suffers from low graphene yield. To address this, one can extend sonication time or introduce a base like NaOH [21]. Nevertheless, prolonged sonication increases defects, necessitating a balance between sonication time and defect minimization [22]. Surfactants play a crucial role in stabilizing graphene dispersion during synthesis, mitigating defects [23]. They serve as the stabilizer, ensuring that graphene remains dispersed in the solution [24].

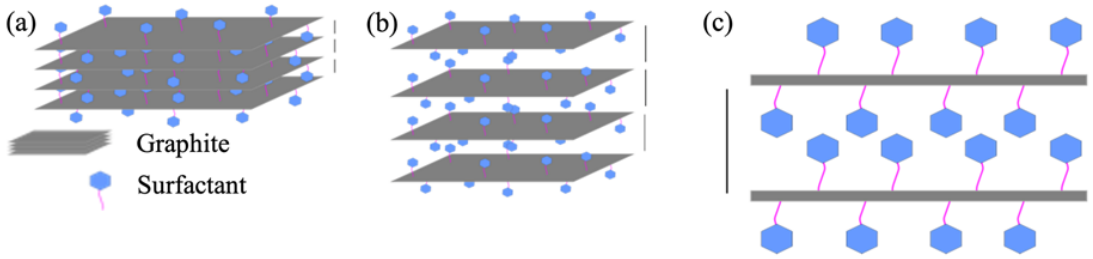


**Figure 1.** Synthesized graphene in LPE method (a) surfactant molecule inside graphitic sheet; (b) distance between graphene sheet increase; and (c) surfactant molecule interaction with graphene.

This work focuses on synthesizing graphene through LPE with minimal sonication time and thermal energy to reduce defects. The resulting graphene will be employed as electrodes in a supercapacitor cell. A key aspect of this investigation is exploring the impact of temperature variation during graphene synthesis on electrical storage performance. Despite the challenges posed by impurities and defects in large-scale graphene synthesis, this research aims to optimize LPE conditions to enhance supercapacitor performance. By minimizing defects through controlled synthesis parameters, the study seeks to contribute to the development of efficient and environmentally friendly energy storage solutions, harnessing the unique properties of graphene for a sustainable energy future.

## 2. MATERIALS AND METHODS

### *2.1. Materials*

Graphite powder was purchased from a local online marketplace. Polyvinyl alcohol (PVA) was purchased from Sigma Aldrich, and potassium hydroxide (KOH) was purchased from Alfa Kimia.

### *2.2. Methods*

#### *2.2.1. Preparation and Synthesize of Graphene*

Graphene synthesis using the LPE method [13]. One gram of graphite powder was dissolved in 100 ml distilled water, forming a graphite solution. Separately, a 0.2 g of LAS surfactant solution was prepared. A 10 mL of the surfactant solution was mixed with 28 mL of the graphite solution and stirred for 6 h. After applying temperatures of 15, 30, and 90 °C (labelled C15, C30, and C90), the solutions were left overnight. Each solution was then sonicated for 1 h, followed by centrifugation at 3500 rpm for 10 min to collect the liquid graphene.

#### *2.2.2. Preparation of KOH Electrolyte Gel*

KOH electrolyte gel preparation involved heating 0.8 g of PVA in 20 mL of distilled water at 90 °C for 2 h. After reaching transparency, 0.7 g of KOH was added and stirred for an additional hour. The solution was left to settle overnight in a petri dish, forming a gel-like sediment.

#### *2.2.3. Preparation of Graphene Electrode*

Graphene electrodes were prepared by drop-casting 1 mL of liquid graphene onto a 13 mm diameter silver plate and heating it at 50 °C for 1 h. The electrodes, separated by a 3 mm thick KOH electrolyte gel, were encapsulated in a custom polypropylene case (see Supplementary Information).

#### *2.2.4. Material Characterization*

Graphene was characterized using optical technique, namely UV-Vis spectroscopy (Shimadzu UV-2400 series, wavelength 200–800 nm with step of 0.5 nm) and Raman spectroscopy (custom-made from Thunder Optic using laser 532 nm). Furthermore, the electrical conductivity of graphene is measure by performing a four-point probe measurement (Keithley USB2400 instrument), using equations 1 and 2 [25].

$$\rho = 2\pi s \frac{V}{I} \quad \textbf{(1)}$$

$$\sigma = \frac{1}{\rho} \quad \textbf{(2)}$$

where $\rho$, $s$ and $\sigma$ are the resistivity ($\Omega m$), distance between probe (m), and the conductivity of the material.

### 2.2.5. Raman Analysis

From the results of Raman spectroscopy measurements, the data were analyzed using the correlation between the $I_D/I_G$ ratsio with in-plane crystalline grain size calculated using the given equation 3 [26].

$$\frac{I_D}{I_G} = C'(\lambda) L_a^2 \quad \textbf{(3)}$$

Where $I_D$, $I_G$, $C'(\lambda)$, and $L_a$ are the intensity of defect, intensity of regularity atomic graphene, constant at excitation wavelength, and in-plane crystalline grain size.

### 2.2.6. Electrochemical Measurement

Cyclic voltammetry (CV) and charging-discharging (CD) measurements (Keithley USB2400) were performed for obtaining the electrochemical properties of the cells. From CV measurement, the specific capacitance was calculated using the following equation 4 [27].

$$C_{sp} = \frac{\int I\, dt}{m\, v\, \Delta V} \quad \textbf{(4)}$$

where $C_{sp}$, $I$, $v$, $m$ are the specific capacitance (F/g), current (A), voltage scan rate (V/s), mass of electrode (g), and voltage window of CV measurement (V), respectively. From CD measurement, an equivalent circuit analysis was applied to obtain electrochemical properties of the cell by fitting the data [28]. Furthermore, the Ragone plot, which describes the relationship between energy density $E_{sp}$ and power density $P_{sp}$, can be plot using the given equations 5 and 6 [29].

$$E_{sp} = \frac{1}{2} C_{sp} V \quad \textbf{(5)}$$

$$P_{sp} = \frac{E_{sp}}{t} \quad \textbf{(6)}$$

with V is the voltage window (V) and t is time.

## 3. RESULTS AND DISCUSSIONS

In this work, graphene was synthesized using LPE method, initiated by dissolving a specific amount of graphite and surfactants. This process aims to create a homogeneous solution of graphite and surfactants. Each solution was stirred for 6 h to allow the surfactant molecules to interact more effectively with the graphitic layers, thereby weakening the interlayer bonds (Fig. 1(b)). The solution was then left overnight. The large-sized graphite (bulk) settles at the bottom of the container, while graphene sheet with a smaller number of sheets (few layers) floated in the surfactant solution. The solutions were sonicated to further weaken and break the bonds between graphene layers that had already been affected by

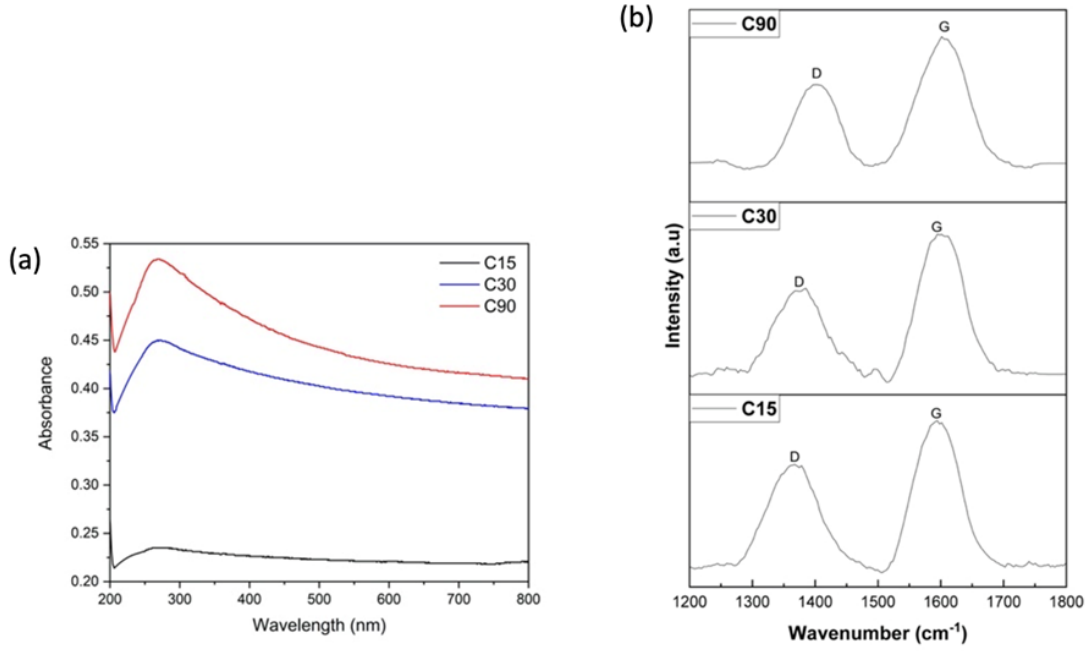


**Figure 2.** Spectrum characterization material graphene from (a) UV-Vis and (b) Raman spectroscopies.

**Table 1.** Parameter D band, G band and $I_D/I_G$ from raman spectrum.

| Sample | D band ($cm^{-1}$) | Int (a.u) | G band ($cm^{-1}$) | Int (a.u) | $I_D/I_G$ |
|---|---|---|---|---|---|
| **C15** | 1374 | 0.00121 | 1608 | 0.00207 | 0.5845 |
| **C30** | 1367 | 0.00264 | 1594 | 0.00413 | 0.6392 |
| **C90** | 1401 | 0.00284 | 1601 | 0.00338 | 0.8402 |

the surfactant interactions (Fig. 1(c)). It can be inferred that longer sonication times lead to more bonds being broken, resulting in a greater degree of exfoliation and more graphene sheets being separated. To re-separate graphene sheets based on their number of sheets, centrifugation is performed. This process separated graphene sheets with fewer layers from those with more layers. In this study, the number of graphene sheets is not studied, based on the methods used, it can be assumed that the resulting material primarily consisted of graphene with a small number of layers.

The concentration of LAS surfactant was selected based on prior studies, which showed that LAS is effective in stabilizing graphene dispersion during LPE. LAS's amphiphilic nature enables it to interact with graphene sheets, forming a protective layer that reduces the risk of agglomeration or structural damage during the sonication process. A concentration of 0.2 g of LAS per 100 mL was chosen because it strikes a balance between effective stabilization of the graphene sheets and minimum impurities. Higher surfactant concentrations could leave excessive surfactant residues, negatively impacting the electrical properties of the final product, while lower concentrations might not provide enough stabilization, leading to agglomeration and defects. This concentration was optimized through preliminary experiments, where minimal aggregation and high-quality graphene dispersion were observed. Additionally, LAS plays a crucial role in minimizing defects during sonication by reducing the mechanical stress on graphene sheets. Cavitation forces generated during sonication create bubbles that exert intense pressure, which can lead to structural defect in graphene sheets. By adsorbing onto the graphene surface, LAS helps to cushion this process and prevents excessive fragmentation.

The graphene solution appears transparent, indicating that the graphene has dissolved in liquid phase (see Supplementary Information, Fig. S2). From the UV-Vis spectrum (Fig. 2(a)), the peak absorption appears at 268 nm, which is consistent with the previous study [30]. This peak is a characteristic feature of graphene, associated with the electron transition from π-π* band and many-body resonant exitonic effect [31]. As the temperature of synthesized graphene ($T_{gs}$)

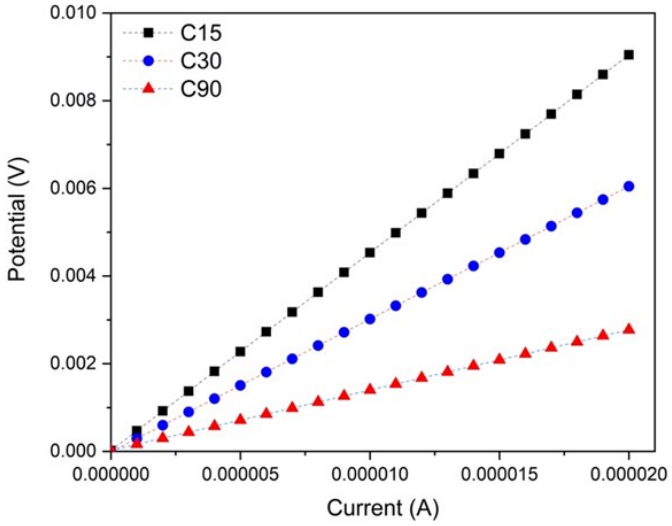


**Figure 3.** Conductivity measurement of graphene.

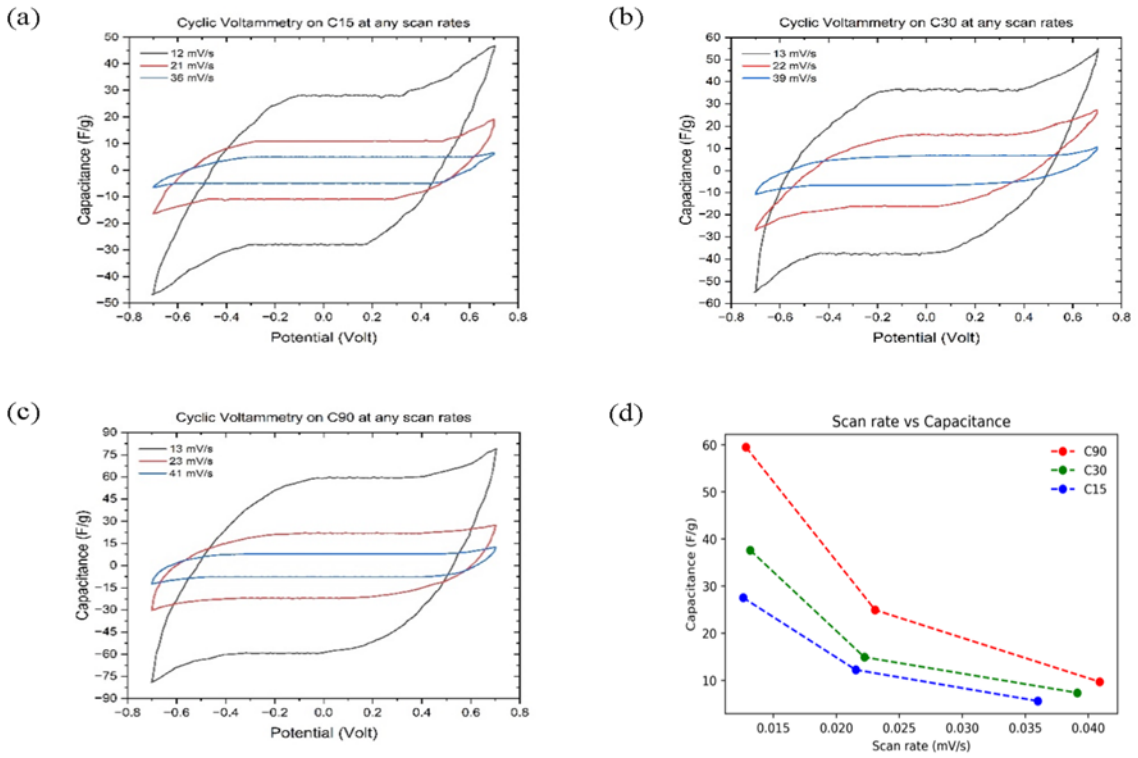


**Figure 4.** Cyclic voltammetry curve of supercapacitor cell using 1.3 M KOH electrolyte gel on sample (a) C15; (b) C30; (c) C90 at any scan rates; and (d) Specific capacitance of each supercapacitor cell from CV curve calculation from different scan rates.

increases, the absorption peak at 270 nm also increases. This is attributed to the improvement in the graphitic structure as $T_{gs}$ increase, resulting in a better electronic structure, approaching that of intrinsic graphene [32].

The formation of intrinsic graphene is further confirmed by the Raman shift data (Fig. 2(b)). The Raman properties of synthesized LPE-graphene are summarized in Table 1. The D and G peaks for C90 occur at approximately 1401 and 1601 $cm^{-1}$, respectively, which are close to the reference (1350 and 1580 $cm^{-1}$) [33]. The intensity of D band ($I_D$) reflects the level of irregularity in the atomic structure of the graphene sheet [34], which may be caused by defects in the carbon atoms structure, such as benzene ring, missing atoms in the lattice, or specific edge patterns like armchair and zigzag configurations [35][36]. Edge defects arise due to the increased number of graphene flakes after the sonication process, where the initially large material is split, separated, and exfoliated into smaller parts [34][37]. The G peak represents the first-order scattering mode $E_{2g}$, while its intensity ($I_G$) indicates the degree of regularity in the atomic structure. The intensity ratio of $I_D$ and $I_G$ ($I_D/I_G$) is commonly used to assess the quality of graphene material [32]. Using equation 3 and Table 1, the increase in $I_D/I_G$ with higher $T_{gs}$ suggests that the number of $sp^2$-ordered rings, which correlates with the in-plane crystalline grain size, also increased [26].

The increase in the $I_D/I_G$ ratio observed in the Raman spectra with higher synthesis temperatures suggests fewer defects and larger crystalline grain sizes. As temperature increases, graphene flakes become more ordered and aligned into larger

**Table 2.** Conductivity and resistivity of graphene with different temperatures on synthesis.

| Variable | C15 | C30 | C90 |
|---|---|---|---|
| $\rho\ (\Omega.m)$ | 5.67 | 3.80 | 1.73 |
| $\sigma(\Omega^{-1}m^{-1})$ | 0.18 | 0.26 | 0.58 |

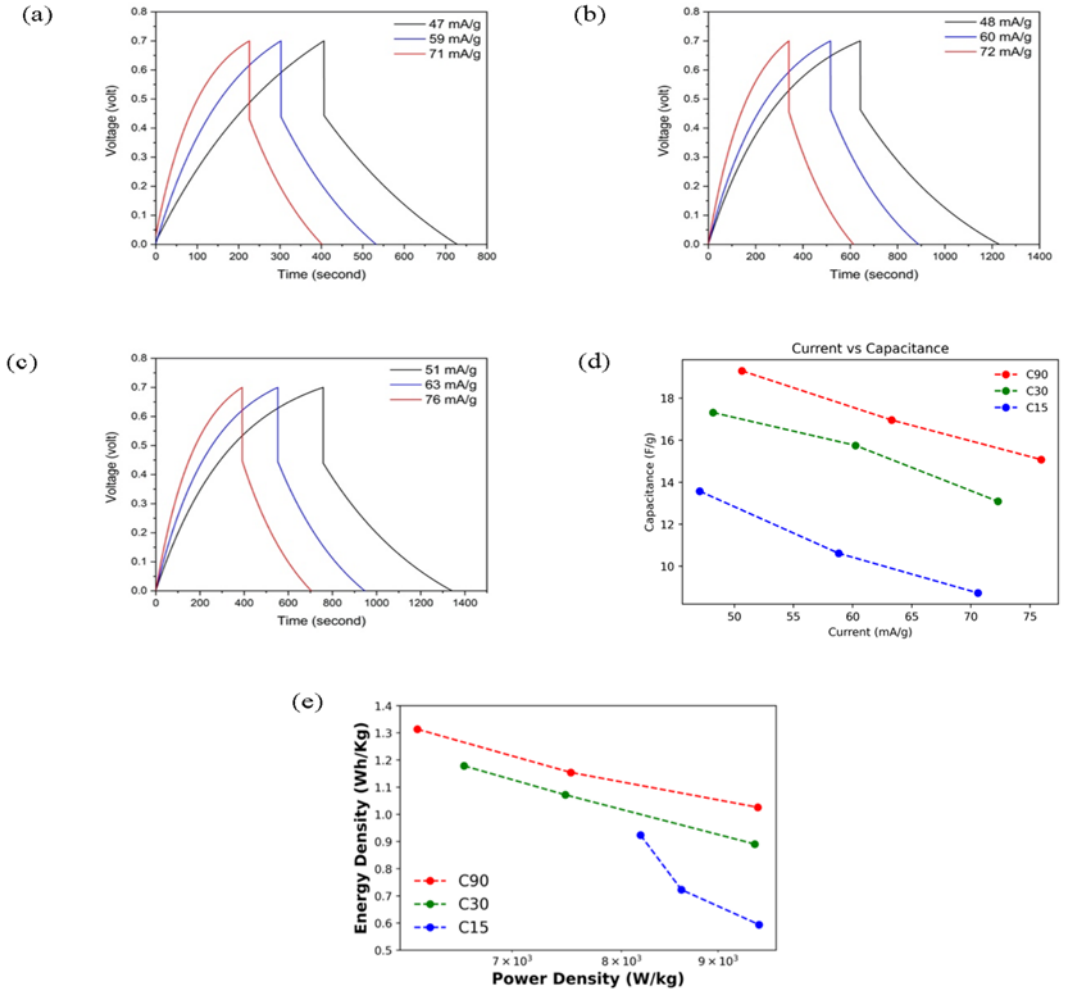


**Figure 5.** Charging-discharging measurement of supercapacitor cell using 1.3 M KOH electrolyte gel (a) C15; (b) C30; (c) C90; (d) Specific capacitance of each supercapacitor cell from CD curve calculation from different current; and (e) Ragone plot.

crystalline domains, which enhances the material's grain size and reduces defect density [38]. The increase in grain size at higher temperatures can be attributed to the increased mobility of atoms, which allows the graphene sheets to align more effectively, forming larger and more ordered structures. This is consistent with previous studies that demonstrate the positive effect of higher temperatures on the crystallinity and grain size of graphene materials.

This indirectly results in an increasingly large surface area of graphene sheet [26]. Fig. 3 shows the result of conductivity measurement using the four-point probe method. The conductivity ($\sigma$) increased as the $T_{gs}$ raised indicating that the graphene produced is more conductive. The electrical properties of synthesized LPE-graphene are summarized in Table 2. Resistivity ($\rho$) and $\sigma$ values are intrinsic values of materials that do not depend on geometry (size) [17]. The increase in conductivity with synthesis temperature is likely due to the reduction of defects and improved crystalline order, as indicated by the Raman spectroscopy data. This leads to better electron transport within the graphene sheets, which in turn enhances the specific capacitance.

The results of CV measurement are shown in Fig. 4(a)-4(c). The CV curve deviates from the ideal rectangular shape, which may be attributed to factors such as electrolyte degradation, slow ion diffusion, or resistive losses in the system. No significant peaks or humps suggest that pseudo-capacitance is not a major contributor to the observed behavior. This shape, representing the

pseudo capacitance effect, is caused by the presence of faradaic reactions in capacitors [37][39], due to the low scan rate (~13 mV/s in our case). The gravimetric capacitance of our supercapacitor increased as $T_{gs}$ is raised. This may be attributed to the larger size of graphene sheets, as the collection of grain increases, as indicated by $I_D/I_G$ value from Raman shift data. The CD measurement can also be used to determine the capacitance of the capacitor (Fig. 5(a)-5(c)). The fact that the CD curve is not symmetric triangle shape indicates that our capacitor is not ideal. This non-ideality may result from possible voltage drop and electrolyte degradation, leading to inefficient charge transfer [40]-[42]. The presence of internal resistance (both equivalent series resistance (ESR) and leakage resistance) contributes to the voltage drop seen in the charging and discharging curves. In this case, several factors are : (1) These resistive elements reduce the efficiency of the capacitor and affect the shape of the CV curve, making it deviate from the ideal rectangular form. (2) Over time, the electrolyte may degrade, particularly at high temperatures during synthesis, reducing its ionic conductivity. This degradation leads to slower ion movement and incomplete charge transfer at the electrode-electrolyte interface, further contributing to non-ideal behavior. (3) The electrode surfaces may not be perfectly uniform, which can result in uneven ion distribution during charge and discharge cycles. This could explain the slight distortions in the CV and CD curves, where ideal capacitor behavior would show more symmetric charge-discharge cycles. (4) The low scan rates (~13 mV/s) used in the CV measurements may highlight limitations in ion diffusion, especially if the ions in the electrolyte struggle to penetrate deep into the porous structure of the graphene electrodes. This would lead to slower charging and discharging, contributing to non-ideal behavior.

It is important to note that the capacitance value is obtained by fitting the CD curve using an equation that provides fitting parameters such as ESR, leakage resistance (Rlk), and capacitance (C). The details of the fitting results can be found in the Supporting Information. Upon closer examination, the scan rate values of the CV and CD measurements for each synthesized graphene sample using LPE method at different temperatures are not identical. This is because the scan rate is not directly set during the measurement but is a result of the tool's reading, leading to variations in the values. Additionally, energy density and power density are crucial in evaluating supercapacitor performance, as illustrated by the Ragone plot (Fig. 5(e). In our measurement, Ragone plot shifts to the top right, indicating that variations in $T_{gs}$ further enhance the charge storage capacity. The Ragone plot (Fig. 5(e)) shows the relationship between energy density and power density for the different samples. As the synthesis temperature increases, the energy and power densities improve due to the higher conductivity and reduced internal resistance. This is reflected in the shift of the plot toward higher values on both axes, indicating that the supercapacitors synthesized at higher temperatures (e.g., 90 °C) exhibit better performance.

As the synthesis temperature increases, the graphene produced shows fewer defects, as confirmed by the Raman spectroscopy data (ID/IG ratio). The reduction in defects enhances the overall crystallinity of the graphene sheets, resulting in improved electrical conductivity. Higher temperatures promote better exfoliation of the graphene layers and lead to more orderly arrangements of the $sp^2$ carbon atoms, which increases the electron mobility across the graphene sheets. The increase in conductivity is directly related to the improvement in the specific capacitance of the supercapacitor. A higher conductivity allows for more efficient charge transport within the electrode material, which in turn enables faster charging and discharging of the supercapacitor. This results in higher specific capacitance values, as more charges can be stored and released in each time frame.

Several studies have explored the use of KOH electrolytes and LPE for fabricating graphene-based supercapacitors. Abdillah et al. demonstrated that electrochemical LPE with 1 M KOH resulted in a high specific capacitance of 116.04 F/g, showcasing KOH's superior ion transfer properties compared to other alkaline electrolytes [43]. Edison et al. achieved a capacitance of 84.82 F/g and an energy density of 3.03 Wh/kg using electrochemical exfoliation with 2 M KOH, highlighting the electrolyte's efficiency for symmetric supercapacitors [44]. In comparison, this research

using ultrasonic LPE and KOH gel electrolyte demonstrated a capacitance of 59 F/g and an energy density of 1.3 Wh/kg, further contributing to the understanding of KOH's effectiveness in energy storage applications.

## 4. CONCLUSIONS

In summary, we have synthesized graphene electrodes via the LPE method with the variation of synthesis temperatures. The Raman spectroscopy indicated $I_D/I_G$ increased with the rising temperature, indicating the larger grain sizes. The CV and CD measurements revealed the enhancement of capacitance with the higher synthesis temperatures. Notably, the graphene electrode synthesized at 90 °C exhibited the highest specific capacitance of 59 F/g at a 13 mV/s scan rate in a 1.3 M KOH electrolyte gel. Hence, the proposed method of preparing graphene using LPE with a green surfactant shows potential for producing high-quality graphene that can serve as a promising electrode material for supercapacitors.

## AUTHOR INFORMATION


### Corresponding Author

**Iman Santoso** — Department of Physics, Universitas Gadjah Mada, Yogyakarta-55281 (Indonesia);
orcid.org/0000-0003-2695-8965
Email: iman.santoso@ugm.ac.id

### Authors

**Buky Wahyu Pratama** — Department of Physics, Universitas Gadjah Mada, Yogyakarta-55281 (Indonesia);
orcid.org/0000-0002-4962-5226

**Haris Suhendar** — Department of Physics, Universitas Negeri Jakarta, Jakarta-13220 (Indonesia);
orcid.org/0000-0001-6385-6090

**Wipsar Sunu Brams Dwandaru** — Department of Physics, Universitas Negeri Yogyakarta, Yogyakarta-55281 (Indonesia);
orcid.org/0000-0002-9692-4640


### Author Contributions

Conceptualization, B. W. P.; Methodology, B. W. P.; Software, H. S.; Validation, B. W. P. and I. S.; Formal Analysis, B. W. P.; Investigation, I. S. and W. S. B.; Resources, B. W. P.; Data Curation, B. W. P., H. S., and I. S.; Writing – Original Draft Preparation, B. W. P.; Writing – Review & Editing, I. S. and W. S. B.; Visualization, B. W. P.; Supervision, I. S. and W. S. B.; Funding Acquisition, B. W. P.

### Conflicts of Interest

The authors declare no conflict of interest.

## SUPPORTING INFORMATION

Supplementary data associated with this article can be found in the online version at doi: 10.47352/jmans.2774-3047.254

## ACKNOWLEDGEMENT

This research was supported by Indonesian Endowment Fund for Education (Lembaga Pengelola Dana Pendidikan (LPDP)) for providing scholarship and financial support [LOG-8575/LPDP.3/2024].

## REFERENCES


[1] H. Yang, S. Kannappan, A. S. Pandian, J. H. Jang, Y. S. Lee, and W. Lu. (2017). "Graphene supercapacitor with both high power and energy density". *Nanotechnology*. **28** (44): 445401. 10.1088/1361-6528/aa8948.

[2] W. Raza, F. Ali, N. Raza, Y. Luo, K.-H. Kim, J. Yang, S. Kumar, A. Mehmood, and E. E. Kwon. (2018). "Recent advancements in supercapacitor technology". *Nano Energy*. **52** : 441-473. 10.1016/j.nanoen.2018.08.013.

[3] C. Portet, P. L. Taberna, P. Simon, E. Flahaut, and C. Laberty-Robert. (2005). "High power density electrodes for Carbon supercapacitor applications". *Electrochimica Acta*. **50** (20): 4174-4181. 10.1016/j.electacta.2005.01.038.

[4] E. Y. L. Teo, L. Muniandy, E.-P. Ng, F. Adam, A. R. Mohamed, R. Jose, and K. F. Chong. (2016). "High surface area activated carbon from rice husk as a high performance supercapacitor electrode". *Electrochimica*

*Acta.* **192** : 110-119. 10.1016/j.electacta.2016.01.140.

[5] G. Ning, Z. Fan, G. Wang, J. Gao, W. Qian, and F. Wei. (2011). "Gram-scale synthesis of nanomesh graphene with high surface area and its application in supercapacitor electrodes". *Chemical Communications.* **47** (21): 5976-8. 10.1039/c1cc11159k.

[6] M. D. Stoller, S. Park, Y. Zhu, J. An, and R. S. Ruoff. (2008). "Graphene-based ultracapacitors". *Nano Letters.* **8** (10): 3498-502. 10.1021/nl802558y.

[7] H. Chen, M. B. Müller, K. J. Gilmore, G. G. Wallace, and D. Li. (2008). "Mechanically Strong, Electrically Conductive, and Biocompatible Graphene Paper". *Advanced Materials.* **20** (18): 3557-3561. 10.1002/adma.200800757.

[8] M. S. A. Bhuyan, M. N. Uddin, M. M. Islam, F. A. Bipasha, and S. S. Hossain. (2016). "Synthesis of graphene". *International Nano Letters.* **6** (2): 65-83. 10.1007/s40089-015-0176-1.

[9] N. I. Zaaba, K. L. Foo, U. Hashim, S. J. Tan, W.-W. Liu, and C. H. Voon. (2017). "Synthesis of Graphene Oxide using Modified Hummers Method: Solvent Influence". *Procedia Engineering.* **184** : 469-477. 10.1016/j.proeng.2017.04.118.

[10] K. E. Whitener and P. E. Sheehan. (2014). "Graphene synthesis". *Diamond and Related Materials.* **46** : 25-34. 10.1016/j.diamond.2014.04.006.

[11] B. Deng, Z. Liu, and H. Peng. (2019). "Toward Mass Production of CVD Graphene Films". *Advanced Materials.* **31** (9): e1800996. 10.1002/adma.201800996.

[12] C. Knieke, A. Berger, M. Voigt, R. N. K. Taylor, J. Röhrl, and W. Peukert. (2010). "Scalable production of graphene sheets by mechanical delamination". *Carbon.* **48** (11): 3196-3204. 10.1016/j.carbon.2010.05.003.

[13] R. Singh and C. C. Tripathi. (2016). "Flexible Supercapacitors using Liquid Phase Exfoliated Graphene with Enhanced Specific Capacitance". *International Journal of Electrochemical Science.* **11** (7): 6336-6346. 10.20964/2016.07.18.

[14] L. Stobinski, B. Lesiak, A. Malolepszy, M. Mazurkiewicz, B. Mierzwa, J. Zemek, P. Jiricek, and I. Bieloshapka. (2014). "Graphene oxide and reduced graphene oxide studied by the XRD, TEM and electron spectroscopy methods". *Journal of Electron Spectroscopy and Related Phenomena.* **195** : 145-154. 10.1016/j.elspec.2014.07.003.

[15] P. Pokharel, S. H. Lee, and D. S. Lee. (2015). "Thermal, Mechanical, and Electrical Properties of Graphene Nanoplatelet/ Graphene Oxide/ Polyurethane Hybrid Nanocomposite". *Journal of Nanoscience and Nanotechnology.* **15** (1): 211-4. 10.1166/jnn.2015.8353.

[16] S. Stankovich, D. A. Dikin, R. D. Piner, K. A. Kohlhaas, A. Kleinhammes, Y. Jia, Y. Wu, S. T. Nguyen, and R. S. Ruoff. (2007). "Synthesis of graphene-based nanosheets via chemical reduction of exfoliated graphite oxide". *Carbon.* **45** (7): 1558-1565. 10.1016/j.carbon.2007.02.034.

[17] H. Suhendar, A. Kusumaatmaja, K. Triyana, and I. Santoso. (2017). "Effect of Chemical Reduction Temperature on Optical Properties of Reduced Graphene Oxide (rGO) and its Potentials Supercapacitor Device". *Materials Science Forum.* **901** : 55-61. 10.4028/www.scientific.net/MSF.901.55.

[18] H. A. Becerril, J. Mao, Z. Liu, R. M. Stoltenberg, Z. Bao, and Y. Chen. (2008). "Evaluation of solution-processed reduced graphene oxide films as transparent conductors". *ACS Nano.* **2** (3): 463-70. 10.1021/nn700375n.

[19] C. Xu, R.-s. Yuan, and X. Wang. (2014). "Selective reduction of graphene oxide". *New Carbon Materials.* **29** (1): 61-66. 10.1016/s1872-5805(14)60126-8.

[20] A. Ciesielski and P. Samori. (2014). "Graphene via sonication assisted liquid-phase exfoliation". *Chemical Society Reviews.* **43** (1): 381-98. 10.1039/c3cs60217f.

[21] W. W. Liu and J. N. Wang. (2011). "Direct exfoliation of graphene in organic solvents with addition of NaOH". *Chemical Communications.* **47** (24): 6888-90. 10.1039/c1cc11933h.

[22] Z. Baig, O. Mamat, M. Mustapha, A. Mumtaz, K. S. Munir, and M. Sarfraz. (2018). "Investigation of tip sonication effects on structural quality of graphene nanoplatelets (GNPs) for superior solvent dispersion". *Ultrasonics Sonochemistry.* **45** : 133-149. 10.1016/j.ultsonch.2018.03.007.

[23] K. Zhang, L. Mao, L. L. Zhang, H. S. On Chan, X. S. Zhao, and J. Wu. (2011). "Surfactant-intercalated, chemically reduced graphene oxide for high performance supercapacitor electrodes". *Journal of Materials Chemistry.* **21** (20). 10.1039/c1jm00007a.

[24] B. W. Pratama and W. S. B. Dwandaru. (2020). "Synthesis of reduced graphene oxide based on thermally modified liquid-phase exfoliation". *Nano Express.* **1** (1). 10.1088/2632-959X/ab8685.

[25] M. Yamashita and M. Agu. (1984). "Geometrical Correction Factor for Semiconductor Resistivity Measurements by Four-Point Probe Method". *Japanese Journal of Applied Physics.* **23** (11R). 10.1143/jjap.23.1499.

[26] A. C. Ferrari and J. Robertson. (2000). "Interpretation of Raman spectra of disordered and amorphous carbon". *Physical Review B.* **61** (20): 14095-14107. 10.1103/PhysRevB.61.14095.

[27] P. Hao, Z. Zhao, Y. Leng, J. Tian, Y. Sang, R. I. Boughton, C. P. Wong, H. Liu, and B. Yang. (2015). "Graphene-based nitrogen self-doped hierarchical porous carbon aerogels derived from chitosan for high performance supercapacitors". *Nano Energy.* **15** : 9-23. 10.1016/j.nanoen.2015.02.035.

[28] S. Ban, J. Zhang, L. Zhang, K. Tsay, D. Song, and X. Zou. (2013). "Charging and discharging electrochemical supercapacitors in the presence of both parallel leakage process and electrochemical decomposition of solvent". *Electrochimica Acta.* **90** : 542-549. 10.1016/j.electacta.2012.12.056.

[29] P.-p. Chang, C.-y. Wang, T. Kinumoto, T. Tsumura, M.-m. Chen, and M. Toyoda. (2018). "Frame-filling C/C composite for high-performance EDLCs with high withstanding voltage". *Carbon.* **131** : 184-192. 10.1016/j.carbon.2018.02.022.

[30] Y.-L. Xu, H.-X. Li, C.-B. Zhou, X.-S. Xiao, Z.-C. Bai, Z.-P. Zhang, and S.-J. Qin. (2020). "The ultraviolet absorption of graphene in the Tamm state". *Optik.* **219**. 10.1016/j.ijleo.2020.165015.

[31] L. Du, S. Wang, D. Scarabelli, L. N. Pfeiffer, K. W. West, S. Fallahi, G. C. Gardner, M. J. Manfra, V. Pellegrini, S. J. Wind, and A. Pinczuk. (2018). "Emerging many-body effects in semiconductor artificial graphene with low disorder". *Nature Communications.* **9** (1): 3299. 10.1038/s41467-018-05775-4.

[32] S. Vadukumpully, J. Paul, and S. Valiyaveettil. (2009). "Cationic surfactant mediated exfoliation of graphite into graphene flakes". *Carbon.* **47** (14): 3288-3294. 10.1016/j.carbon.2009.07.049.

[33] A. Das, B. Chakraborty, and A. K. Sood. (2008). "Raman spectroscopy of graphene on different substrates and influence of defects". *Bulletin of Materials Science.* **31** (3): 579-584. 10.1007/s12034-008-0090-5.

[34] F. M. Casallas-Caicedo, E. Vera-López, A. Agarwal, V. Drozd, A. Durigin, and C. Wang. (2019). "Effect of exfoliation method on graphite oxide. A comparison between exfoliation by ball milling and sonication in different media". *Journal of Physics: Conference Series.* **1386** (1). 10.1088/1742-6596/1386/1/012016.

[35] 2012)." Graphene Nanoelectronics. 10.1007/978-3-642-22984-8.

[36] S. M. Notley. (2012). "Highly concentrated aqueous suspensions of graphene through ultrasonic exfoliation with continuous surfactant addition". *Langmuir.* **28** (40): 14110-3. 10.1021/la302750e.

[37] J. R. Miller, R. A. Outlaw, and B. C. Holloway. (2011). "Graphene electric double layer capacitor with ultra-high-power performance". *Electrochimica Acta.* **56** (28): 10443-10449. 10.1016/j.electacta.2011.05.122.

[38] I. Santoso, R. S. Singh, P. K. Gogoi, T. C. Asmara, D. Wei, W. Chen, A. T. S. Wee, V. M. Pereira, and A. Rusydi. (2014). "Tunable optical absorption and interactions in

graphene via oxygen plasma". *Physical Review B.* **89** (7). 10.1103/PhysRevB.89.075134.

[39] E. Frackowiak and F. Béguin. (2001). "Carbon materials for the electrochemical storage of energy in capacitors". *Carbon.* **39** (6): 937-950. 10.1016/s0008-6223(00)00183-4.

[40] B. Hsia. (2013). "Materials synthesis and characterization for micro-supercapacitor applications". University of California, Berkeley.

[41] X. Sun, X. Zhang, H. Zhang, D. Zhang, and Y. Ma. (2012). "A comparative study of activated carbon-based symmetric supercapacitors in Li2SO4 and KOH aqueous electrolytes". *Journal of Solid State Electrochemistry.* **16** (8): 2597-2603. 10.1007/s10008-012-1678-7.

[42] L. Guan, L. Yu, and G. Z. Chen. (2016). "Capacitive and non-capacitive faradaic charge storage". *Electrochimica Acta.* **206** : 464-478. 10.1016/j.electacta.2016.01.213.

[43] O. B. Abdillah, A. H. Aimon, and F. Iskandar. (2022). "Electrolyte-dependent Specific Capacitance and Charge Transfer Properties of Exfoliated Graphene as an Electrode of Supercapacitor". the 2022 7th International Conference on Electric Vehicular Technology (ICEVT). 10.1109/ICEVT55516.2022.9924637.

[44] T. N. J. I. Edison, R. Atchudan, N. Karthik, P. Chandrasekaran, S. Perumal, P. Arunachalam, P. B. Raja, M. G. Sethuraman, and Y. R. Lee. (2021). "Electrochemically exfoliated graphene sheets as electrode material for aqueous symmetric supercapacitors". *Surface and Coatings Technology.* **416**. 10.1016/j.surfcoat.2021.127150.